Relaxation and coarsening of weakly-interacting breathers in a simplified DNLS chain

Stefano Iubini[1,2], **Antonio Politi**[3], **Paolo Politi**[4,2]

[1] Dipartimento di Fisica e Astronomia, Università di Firenze, via G. Sansone 1 I-50019, Sesto Fiorentino, Italy
[2] Istituto Nazionale di Fisica Nucleare, Sezione di Firenze, via G. Sansone 1 I-50019, Sesto Fiorentino, Italy
[3] Institute for Complex Systems and Mathematical Biology & SUPA University of Aberdeen, Aberdeen AB24 3UE, United Kingdom
[4] Istituto dei Sistemi Complessi, Consiglio Nazionale delle Ricerche, via Madonna del Piano 10, I-50019 Sesto Fiorentino, Italy

E-mail: stefano.iubini@unifi.it

Abstract. The Discrete NonLinear Schrödinger (DNLS) equation displays a region of parameters where the presence of discrete breathers slows down the macroscopic dynamics due to their weak interaction with the background. We investigate the properties of this process by invoking a simple stochastic model that allows to tune the interaction between a breather and its neighboring sites.

Keywords: Coarsening processes, Stochastic particle dynamics, Diffusion.

Submitted to: *Journal of Statistical Mechanics: theory and experiment*

1. Introduction

The one dimensional Discrete Non Linear Schrödinger (DNLS) equation [1, 2]

$$i\dot{z}_n = -2|z_n|^2 z_n - \gamma(z_{n+1} + z_{n-1}) \tag{1}$$

with $1 \leq n \leq N$ (and suitable boundary conditions), is a prototype model of wave propagation in nonlinear lattices [3] and provides a reasonably accurate description of several physical setups, ranging from trapped cold gases [4, 5, 6], to optical waveguides [7, 8] and magnetic systems [9, 10, 11]. One of the peculiarities of its dynamics is the existence of a region in the parameter space, where localized excitations, (breathers [12]) spontaneously emerge. If the energy density is large enough, a typical configuration can be decomposed into a background and a certain number of breathers. The background collects most of the mass (norm) and is characterized by a Poissonian distribution of the local amplitude. The breathers, characterized by a fast rotation, host a finite fraction of the energy. This phase is referred to as a negative-temperature regime, because the injection of energy reduces the entropy, as expected for any energy spectrum which is bounded from above, once all levels are equally populated [13].

In the negative temperature region, direct simulations of the DNLS show that, after some transient, the dynamics is essentially frozen [14]. This is in contrast

with the expectation that the density of breathers should decrease in time through a sort of entropic coarsening, where the expected final state is made up of a single breather which absorbs all the excess energy, sitting on top of an infinite-temperature background [15, 16, 17, 18].

In order to understand this discrepancy, several approaches can be adopted, ranging from focused numerical simulations to approximations of the exact DNLS model. Our working hypothesis is to explore the implications of the existence of two conserved quantities: the energy

$$H = \sum_{n=1}^{N} \left[|z_n|^4 + \gamma(z_n^* z_{n+1} + z_n z_{n+1}^*) \right] \tag{2}$$

and the mass

$$A = \sum_n |z_n|^2 \, . \tag{3}$$

Here below, instead of deriving suitable hydrodynamic equations, we prefer to study simple microscopic stochastic models, as they offer better chances of performing analytical calculations. In a previous publication [19] we have already introduced and studied two such models. The first one was introduced by replacing the deterministic coupling present in the DNLS with a local Microcanonical Monte Carlo (MMC) move, which does not break the two general conservation laws (see Fig. 1(a)). Remarkably, the phase diagram of this model, defined through the mass density a and the energy density $u = H/N$, contains a region where breathers are characterized by a slow dynamics. This region is identified by the condition $u > a^2/2$ and coincides with the negative-temperature phase of DNLS for $\gamma \ll 1$.

In the second model, a partial exclusion process (PEP), the space is divided into disjoint channels where particles diffuse according to the exclusion constraint, separated by a set of preselected breather sites which can freely emit and absorb particles (see Fig. 1(b)). The PEP model too exhibits a slow dynamics very similar to that of the MMC model, if the overall density of particles c is larger than $1/2$ [19].

In both models, above the corresponding critical condition, a slow dynamics manifests itself as a sort of coarsening, which has, however, no equivalent in the DNLS, where the dynamics essentially freezes. An important, conceptual difference between the DNLS equation and the two stochastic models is the absence of a phase dynamics in the latter ones. In the original context, the local variable is indeed $z_n := \sqrt{a_n} \mathrm{e}^{i\phi_n}$, while only a_n is for instance present in the MMC. From the point of view of nonlinear dynamics this is quite awkward, since the phase is quite sensitive to coupling, to the extent that often the opposite approximation is made: amplitude dynamics is neglected [20]. The approach is, however, justifiable in our context when γ is small: in this limit, neither of the two conserved quantites depends on the phases, so that the physics is contained in the distribution of the amplitudes. Phases enter only in the coupling mechanism, which, in the MMC, has been designed just to capture entropic effects in the simplest possible way. As a result, one can claim that the disagreement between the coarsening dynamics (exhibited by MMC and PEP) and the evolution of breathers in the DNLS can be traced back to the way breather-background interaction is accounted for. More specifically, in the original DNLS, breathers of increasing amplitude rotate faster and faster (the frequency ω of a massive breather is equal to $2|z_n|^2 = 2a_n$). Therefore, the effective coupling, being determined by the average of $\gamma(z_{n+1} + z_{n-1})$, becomes increasingly weak upon increasing a_n. An

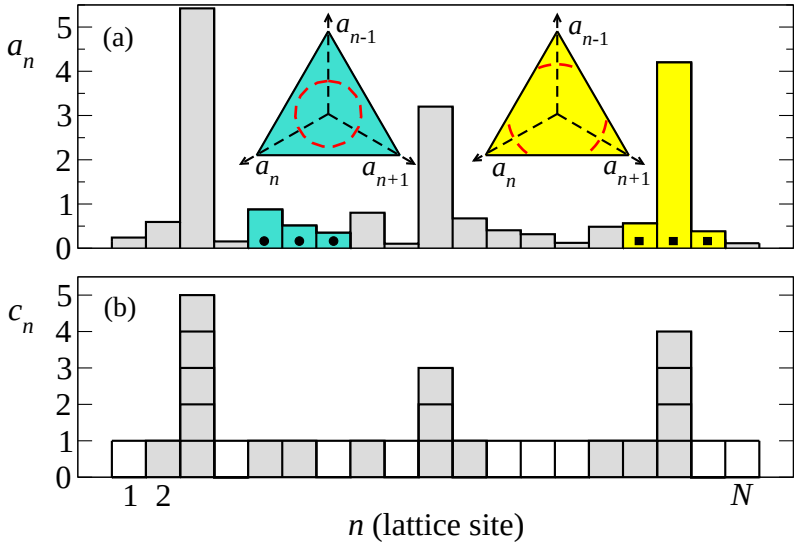

Figure 1. (a): The MMC model. A typical amplitude profile a_n displays a certain number of high-amplitude breathers superposed to a background. Left and right insets show in dashed red lines the available states respectively for a background triplet of sites (turquoise bars marked with black dots) and a triplet containing a breather (yellow bars marked with black squares). The legal configurations are obtained as intersection between a plane (main triangle) and a sphere (not shown) that account for local conservation of mass and energy, respectively. Due to the further constraint on the positivity of the amplitudes a_n, the allowed states may lie on three disconnected arcs, see the right inset. This happens when one of the three amplitudes is significantly larger than the others. (b): The PEP model. The amplitude profile in panel (a) is reproduced in terms of the integer amplitude c_n. White and grey squares highlight respectively empty ($c_n = 0$) and occupied ($c_n > 0$) sites.

explicit perturbative analysis of the DNLS is a subtle object that is currently under investigation. Here, we focus on simple stochastic models, where we have a full control of the evolution rule.

The weakening of the interaction induced by an increasingly fast rotation is here simulated by postulating that the coupling strength depends on the breather amplitude. More precisely, we introduce the probability $\alpha \in (0, 1]$ for a move involving the breather to actually occur. After investigating the case of constant α (in order to test the correct scaling) we consider $\alpha = h^{-\beta}$, where h is the breather height. One of the major results of this paper concerns the corresponding coarsening exponent $1/\zeta$, defined through the expression $L(t) \sim t^{1/\zeta}$, giving the time evolution of the average distance L between neighbouring breathers. We find

$$\zeta = \begin{cases} 3 & \beta \leq 1 \\ 2 + \beta & \beta > 1 \end{cases} . \tag{4}$$

Altogether, in section 2, we analyse the relaxation of a single breather for fixed small α in the PEP model, finding that the process is initially ballistic, and becomes diffusive at later times. We repeat the study, assuming that α depends on the breather height: a similar scenario is found. In the following section 3, we focus on the interactions between neighbouring breathers, showing that the process is eventually

diffusive. We also connect the value of the diffusion coefficient with the coarsening exponent. In section 4, we analyse some, more natural, coupling schemes in the MMC, finding one which leads to a logarithmically slow process, that would be closer to the scenario actually observed in the DNLS. Finally, in section 5, some conclusions are drawn and the open problems briefly summarized.

2. Relaxation of a single breather

In this section we study the PEP model defined on a lattice of N sites with periodic boundary conditions, see Fig. 1(b). The variable c_n identifies the number of particles in the site n, which can be of background or breather type. In the former case, the particles diffuse as in a standard exclusion process, i.e. c_n can be at most equal to 1. The breathers are "reservoirs" ($c_n > 1$) which exchange particles with neighbouring (background) sites. If the breather content reduces to just a single particle, $c_n = 1$, it becomes a background site for ever. The evolution rule is simple: we randomly choose an ordered pair of neighbouring sites (i, j), $j = i \pm 1$, and make the move $(c_i, c_j) \to (c_i - 1, c_j + 1)$ if and only if $c_i > 0$ and $c_j \neq 1$. This means that we move a particle if it exists and it enters either an empty background ($c_j = 0$), or a breather site ($c_j > 1$). If the move involves a breather (i.e., either $c_i > 1$ or $c_j > 1$), it is accepted with probability α; if it does not, it is always accepted.

At variance with both MMC and the original DNLS, in this model there is only one conserved quantity (the number of particles), but accompanied by an additional constraint in the background, due to the exclusion rule. There is another difference between PEP and MMC/DNLS models: in the former, breather do not arise spontaneously. In fact, according to above rules a breather can be destroyed but it cannot be created. Finally, it is instructive to compare the critical density $c = 1/2$ of the PEP model with the infinite-temperature line $u = a^2/2$ of the MMC. For $T = \infty$, the MMC is characterized by a Poissonian distribution of masses, i.e. $\langle a^2 \rangle - \langle a \rangle^2 = \langle a \rangle^2$. In the PEP model, where a is a binary variable with average c, the above condition writes $c - c^2 = c^2$, whence $c = 1/2$.

In Fig. 2 we report the average evolution of a single breather of initial height $h(0) < N/2$ sitting on an empty background with periodic boundary conditions. The condition on $h(0)$ implies that the breather is eventually absorbed by the background, because the infinite-temperature regime corresponds to an occupation density equal to 1/2. In fact, we have chosen $h(0) = 100$, much smaller than $N = 10^4$, to reduce boundary effects during the breather relaxation. The results show the existence of two regimes separated by a crossover time $t_c \sim 1/\alpha^2$. For short times the average height of the breather decreases ballistically, $\langle \Delta h(t) \rangle \equiv \langle h(0) - h(t) \rangle \simeq \alpha t$, while for large times it decreases diffusionally, $\langle \Delta h(t) \rangle \simeq \sqrt{t}$. At even longer times $\langle \Delta h(t) \rangle$ saturates because of the finite height of the breather, which runs out of particles. The different behavior at short/long times can be qualitatively understood as follows. At early times (especially if α is vanishingly small) released particles freely diffuse in a practically empty background with no mutual interaction and a vanishing probability to be reabsorbed. At long times, emitted particles have a much higher probability to return to the breather.

This argument can be made more rigorous under the approximation of continuous time and space variables. We proceed into two steps, by first deriving a set of mean-field differential equations for the probability $p_n(t)$ that the site n is occupied at time

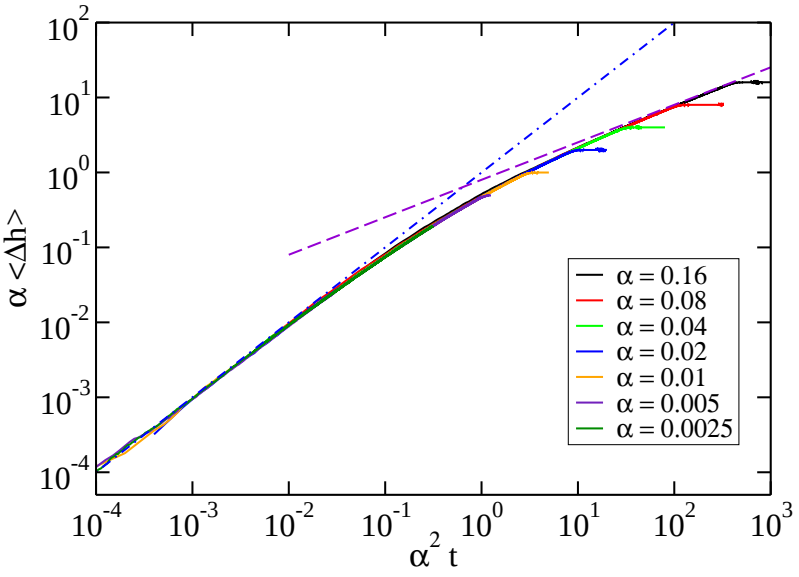

Figure 2. Evolution of the average height variation $\langle h(0) - h(t) \rangle$ of the breather during the relaxation process in rescaled units. Averages have been performed over 2000 different initial conditions. The dotted-dashed blue curve represents the analytical prediction for the ballistic growth, Eq. (12), and the dashed purple curve is the analytic prediction for the diffusive growth, see Eq. (13).

t (the breather being located in the site $n = 0$),

$$\dot{p}_n \equiv \frac{\Delta p_n}{\Delta t} = \frac{1}{2}\left[p_{n-1}(1-p_n) + p_{n+1}(1-p_n) - p_n(1-p_{n-1}) - p_n(1-p_{n+1})\right] = \\ = \frac{1}{2}(p_{n+1} + p_{n-1} - 2p_n) \qquad n > 1 \tag{5}$$

and

$$\dot{p}_1 \equiv \frac{\Delta p_1}{\Delta t} = \frac{1}{2}\left[\alpha(1-p_1) - \alpha p_1 + p_2(1-p_1) - p_1(1-p_2)\right] \\ = \frac{1}{2}\left[\alpha(1-2p_1) + (p_2 - p_1)\right], \tag{6}$$

where $\Delta t = 1$ corresponds to the implementation of N random moves (N is the lattice size). The evolution equation for p_1 can be made formally equivalent to the bulk dynamics (5) upon introducing a p_0 such that

$$\alpha(1-2p_1) + (p_2 - p_1) = (p_0 + p_2) - 2p_1 \ . \tag{7}$$

As a next step, we introduce the continuous variable $x = n - 1$ and the corresponding probability density $\rho(x,t) = p_n - 1/2$, so that the stationary solution is $\rho(x) = 0$. Under the approximation of a weak dependence of ρ on the spatial variable x (which becomes increasingly correct at long times), the bulk dynamics is described by a standard diffusive equation

$$\partial_t \rho(x,t) = D\partial_{xx}\rho(x,t) \ , \tag{8}$$

where $D = 1/2$. Moreover, one can assume‡ $p_0 = \rho(0) + 1/2 - \rho_x(0)$, so that Eq. (7) transforms into the boundary condition

$$\rho_x(0) = 2\alpha\rho(0) \equiv r\rho(0). \tag{9}$$

Therefore, we recover the well known result that the exclusion process is purely diffusive [21] and find that the interaction with the breather can be modelled by a Robin (semi-reflecting) boundary condition in $x = 0^+$, gauged by the variable r. For $\alpha \to \infty$, the Robin condition reduces to a standard absorbing boundary condition, $\rho(0) = 0$, while for $\alpha \to 0$, it corresponds to a reflecting boundary, $\rho_x(0) = 0$. The case $\alpha = 1$, studied in Ref. [19], corresponds to an intermediate setup, characterized by a finite interaction time-scale, because for $\alpha = 1$ attachment occurs on the time scale of diffusion.

We now want to determine the average height reduction $\langle \Delta h(t) \rangle$ of a breather due to the particles that have been emitted but *not yet* reabsorbed. We need to know the probability $F(t)dt$ that a particle is being reabsorbed in the time interval $(t, t + dt)$. This quantity can be evaluated exactly using the continuum model and assuming that a particle is released in $x = x_0$ at $t = 0$ and it is thereby let free to diffuse in $[0, \infty]$. Note that the value of x_0 is not crucial for the continuum model as long as it is chosen to be close to the origin. The analytical expression for $F(t)$ valid for all t is fairly complicated and it is given in Appendix A. Here we limit to give its limiting expression for short and long times,

$$F(t) \simeq \begin{cases} 4\alpha\sqrt{D/(\pi t)} & x_0^2 \ll t \ll \alpha^{-2} \\ 1/(2\alpha\sqrt{\pi D t^3}) & t \gg \alpha^{-2} \end{cases} . \tag{10}$$

The height reduction $\langle \Delta h(t) \rangle$ of the breather is thereby obtained by integrating over all particles that have been emitted and not yet absorbed at time t. However, we must be careful because the evaluation of the number of emitted particles (either reabsorbed or not) is not trivial, since the emission of a particle from the breather is possible only if the neighbouring site which should receive it is empty. Since the initial condition corresponds to an empty background, at short times the probability $(1 - p_1)$ that the neighboring sites are empty is practically equal to 1. On the other hand, at large times, after many emissions of particles, the region around the breather is almost at equilibrium, corresponding to $p_1 = 1/2$. In general, one can write

$$\langle \Delta h(t) \rangle = \alpha \int_0^t dt' (1 - p_1(t')) \int_{t'}^{\infty} dt'' F(t''). \tag{11}$$

Using the limiting expressions for $F(t)$ (provided in Eq. (10)) and for $p_1(t)$ (discussed here above), we find the following two regimes,

$$\langle \Delta h(t) \rangle \simeq \alpha t \qquad x_0^2 \ll t \ll \alpha^{-2} \tag{12}$$

$$\langle \Delta h(t) \rangle \simeq \sqrt{\frac{2t}{\pi}} \qquad t \gg \alpha^{-2}\,, \tag{13}$$

where we have used $D = 1/2$. The details of the derivation of Eqs. (12) and (13) are given in Appendix B. These limiting behaviors are plotted in Fig. 2 and show a very good agreement with numerical simulations.

So far we have considered a constant coupling strength α. We now turn to a more physical case where α varies with the breather height

$$\alpha(h) = h^{-\beta}$$

‡ Let us remind that $\rho(0) + \frac{1}{2}$ corresponds, in the discrete lattice, to p_1.

and β is a real and positive parameter. The dependence of α on h is such that the higher a breather is, the lower is its coupling with the background. This also implies that the effective coupling is implicitly time-dependent. The data obtained for different β-values are reported in Fig. 3, using the same scaling ansatz as before, with the only difference that now, α is referred to the initial amplitude (i.e. $\tilde{\alpha} = \alpha(h(0))$).

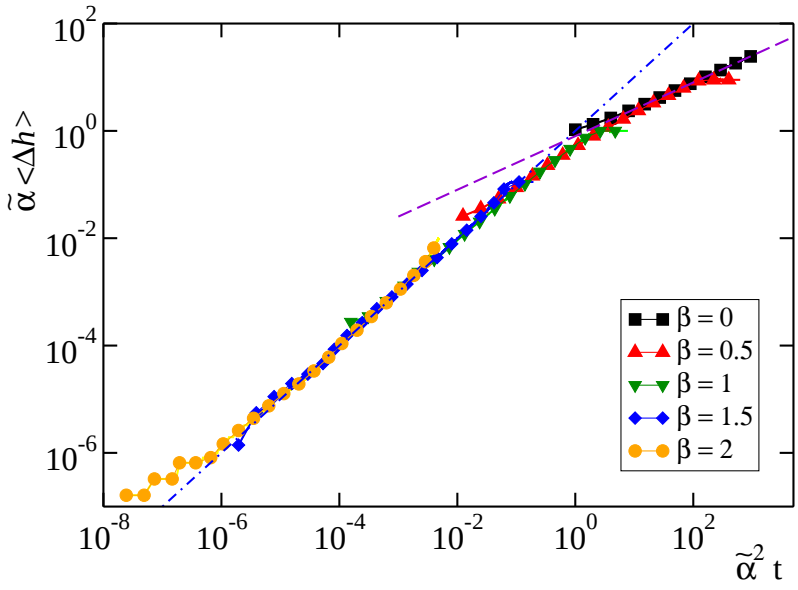

Figure 3. Breather relaxation dynamics for different choices of the coupling exponent β. Simulations refer to a setup with $N = 10000$ lattice sites and a breather with initial height $h(0) = 80$. The PEP channel is initially empty. Data are averaged over 1000 realizations. The dotted-dashed and dashed curves represent the analytical predictions as in Fig. 2, with α replaced by $\tilde{\alpha}$.

3. Breather interactions

Here we are mostly interested in determining the exponent ζ which controls the way the density d_B of breathers decays in time ($d_B \approx t^{-1/\zeta}$). In order to do so, it is first necessary to understand how breathers interact with each other. After some transient, a set of breathers is present, which sit on a background characterized by the occupation density $\rho = 1/2$. Let the origin of the time variable be set at such a stage, when the average distance between neighbouring breathers is L, while their average height is $\overline{h} = kL$, with $k > 0$ (this ensures that the surplus of energy contained in the breathers is an extensive quantity). In these conditions the background is "at equilibrium" at $T = \infty$ and, on average, the breathers do neither absorb nor release particles. However, the particles stochastically emitted can occasionally diffuse and be absorbed by a neighbouring breather. This mechanism couples breathers, which can exchange particles through the background, therefore inducing a diffusion of breathers' height. Let us focus on a couple of breathers with initial height $h(0) = kL$. The square displacement σ^2

$$\sigma^2 \equiv \langle (h(t) - h(0))^2 \rangle \tag{14}$$

is expected to grow as $\sigma^2 = D_B t$, where $D_B(L)$ is the diffusion constant of the exchange process. By definition, one of the two breathers is completely absorbed after a time τ, when $\sigma^2(\tau) \simeq h^2(0)$. Therefore the absorption time τ scales with L as $\tau(L) \simeq h^2(0)/D_B(L)$. In order to determine the coarsening exponent it is necessary to invert the relation $d_B \approx \tau^{-1/\zeta}$, once set $d_B = 1/L$ and $h^2(0) \simeq L^2$. Accordingly,

$$L \simeq \left(\frac{L^2}{D_B}\right)^{1/\zeta} \quad . \tag{15}$$

As a result, the coarsening exponent is fully determined by the scaling of D_B with L.

With reference to the two-breather setup, D_B can be expressed as the product of the rate γ to release a particle tout court by the probability P_c that the particle is absorbed by the neighboring breather (instead of being absorbed back by the emitter). An analytical calculation of P_c is reported in Appendix C for a simple geometry consisting of only two breathers placed at the boundaries of a PEP channel with fixed boundary conditions. For this setup,

$$\gamma = \frac{\alpha}{2}, \qquad P_c(L,\alpha) = \frac{1}{2(1+L\alpha)} \tag{16}$$

and therefore

$$D_B(L,\alpha) = \frac{\alpha}{4(1+L\alpha)}. \tag{17}$$

When α scales with the breather height, i.e. when $\alpha = \bar{h}^{-\beta} = (kL)^{-\beta}$, the above equation provides the relevant scaling of D_B with the system size L. In particular, we find

$$D_B = \begin{cases} \dfrac{S(k,\beta,L)}{L} & \beta \leq 1 \\ \dfrac{S(k,\beta,L)}{L^\beta} & \beta > 1 \end{cases}, \tag{18}$$

where $S(k,\beta,L)$ is a prefactor weakly dependent on L for large L. Explicitly,

$$S(k,\beta,L) = \begin{cases} \dfrac{k^{-\beta}L^{1-\beta}}{4\left(1+k^{-\beta}L^{1-\beta}\right)} & \beta \leq 1 \\ \dfrac{k^{-\beta}}{4\left(1+k^{-\beta}L^{1-\beta}\right)} & \beta > 1 \end{cases} \tag{19}$$

Altogether, from Eq. (16) we finally obtain $\zeta = 3$ for $\beta \leq 1$ and $\zeta = (2+\beta)$ for $\beta > 1$.

In Fig. 4 we show the growth of $\sigma^2(t)$ as obtained by directly simulating the evolution of a PEP model where two breathers are initially superposed to a background in equilibrium at infinite temperature (i.e., with a density 1/2). Horizontal and vertical axes are rescaled so as to collapse data corresponding to different system sizes on a single curve. In all cases, the growth of σ^2 is asymptotically linear: $\sigma^2(t) \sim t/L$ for $\beta = 0$ and $\beta = 1$, while $\sigma^2(t) \sim t/L^2$ for $\beta = 2$, in agreement with the prediction in Eq. (18). A detailed check of the prefactor $S(k,\beta,L)$ extracted from numerical simulations, is presented in Fig. 5, where it is compared with the analytical formula, Eq. (19). An excellent agreement is found.

It is interesting to notice that the asymptotic linear growth of σ^2, which confirms the eventual diffusive behavior of the breather amplitude, may be preceeded by a sub-diffusive behavior, where $\sigma \simeq t^{1/4}$ (see the green dotted curve in Fig. 4). This behaviour can be understood by invoking a somehow unexpected relationship with surface roughening phenomena. Consider a finite PEP extending from site 0, where it

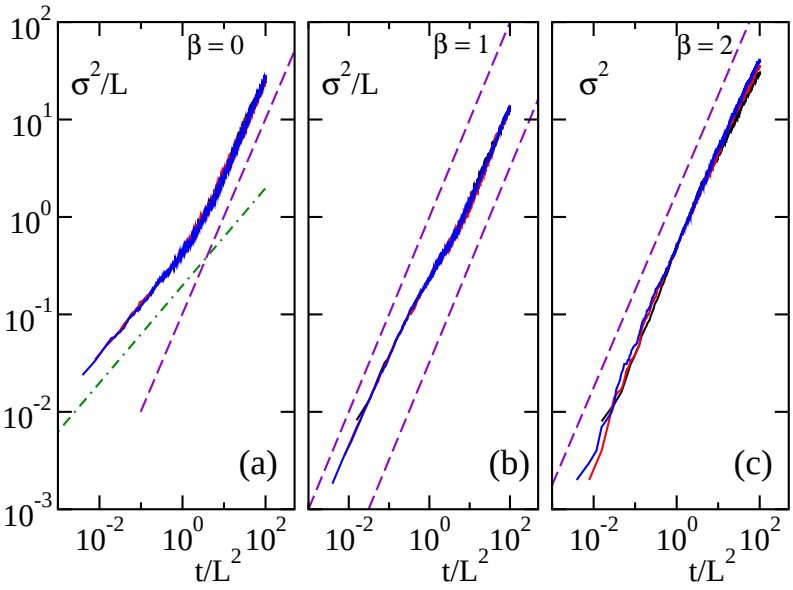

Figure 4. Evolution of the amplitude fluctuations σ^2 of two breathers sitting on an infinite temperature background for different coupling exponents β. Black, red, and blue full lines (indistinguishable) correspond to $N = 64$, 128, and 256, respectively. Data are obtained by averaging over a set of 1000 independent trajectories. The initial condition consists of two breathers of equal amplitude $h(0) = N = L$ at the boundaries of the chain. Dotted-dashed (green) and dashed (purple) lines correspond to a square root and linear increase of σ^2, respectively.

is in contact with a breather, to site L where fixed boundary conditions are imposed. Let $c_i(t)$ be a variable denoting whether a particle is present or not on site i at time t and introduce

$$C_j(t) = \sum_{i \geq j}^{L} c_i(t) \ .$$

The variable $C_j(t)$ counts the number of particles present in the system on the right of the site j. It can be written as $C_j(t) = (L - j)/2 + s_j(t)$, where $s_j(t)$ can be interpreted as a rough interface of vanishing average height. Therefore the fluctuations of $s_0(t)$ (and thereby of $C_0(t)$), represent the fluctuations of the breather height as well as the fluctuations of the rough surface. In the contexts analysed in this paper the bulk dynamics is fully linear, so that it is appropriate to invoke an analogy with the Edwards-Wilkinson model, whose fluctuations are precisely charactrized by the exponent 1/4 [22] seen in Fig. 4 for $\beta = 0$.

This "early time" behavior appears because in between the emission of a particle from a breather and the next emission, the system may not have the time to reach local equilibrium when β is small. $\beta = 1$ is the limiting value for the observation of the initial slow growth. In this critical case, the anomaly reduces to just a different multiplicative coefficient in front of the linear term, see Fig. 4(b).

We conclude this Section with the remark that above derivation of $\tau(L)$ applies to any $\alpha(L)$ dependence so long as it represents a coupling which weakens upon increasing

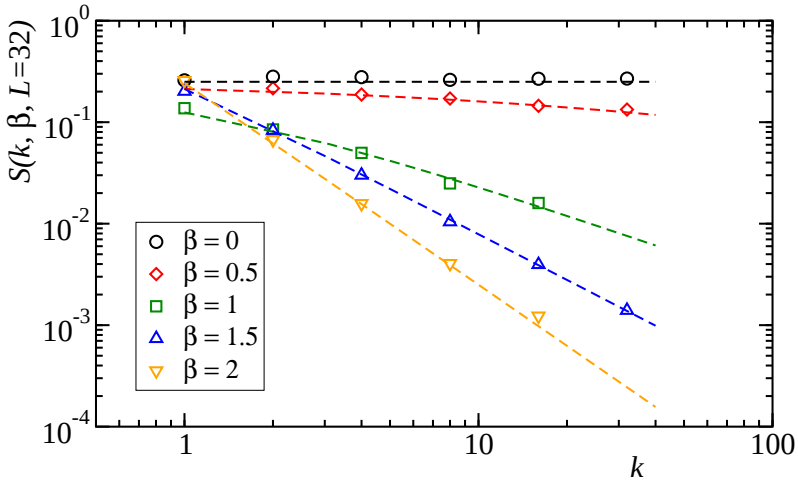

Figure 5. The diffusion prefactor $S(k, \beta, L = 32)$ (open symbols) computed from a fit of the asymptotic growth of $\sigma^2(t)$ for different values of β and k in a chain of $N = 32$ sites. Dashed lines are obtained from the analytical prediction in Eq. (19). Simulations are performed by superposing two breathers with amplitude $h(0) = kL$ at the two boundaries of a PEP chain at infinite temperature and with fixed boundary conditions. The breather interaction probability is $\alpha = h(0)^{-\beta}$. For each choice of k and β , the mean square height displacement σ^2 is computed by averaging over 1000 independent trajectories. The coefficient $S(k, \beta, L = 32)$ is therefore extracted by performing a linear fit of σ^2 in the asymptotic region where $\sigma^2 \sim t$.

the breather height. This includes an exponential dependence, in which case the time required for the death of a breather grows exponentially with its size.

4. The MMC model

Here, we discuss the coarsening process in the MMC setup. As briefly anticipated in the introduction, the evolution rule is a typical microcanonical Monte Carlo move restricted to neighbouring particles, so as to maintain the locality of the interactions of the DNLS equation. In practice, a triplet of neighbouring sites, $(n-1, n, n+1)$, is randomly chosen and the variables (a_{n-1}, a_n, a_{n+1}) updated so as to conserve mass and energy.

The positivity of a_n implies that when a high-mass (breather) site is involved (see Fig. 1(a)), the accessible phase space reduces, to the point that, if a finite mass were concentrated in a single site, the two neighbouring ones being perfectly empty, no redistribution would be possible at all. In the absence of the condition for the mass to be positive, the rule would be equivalent to a stochastic scheme which preserves kinetic energy and linear momentum, of the type used to "ergodize" chains of oscillators [23, 24, 25, 26], where no such exotic phenomena are observed.

The same analysis carried out in the previous sections for the PEP, could be repeated for the MMC, by introducing a suitable height-dependent coupling. We have verified that this leads to the same scenario and, therefore, we do not see a compelling reason to show the corresponding results. We rather propose some considerations which make the weakening assumption less ad hoc than introducing

a priori a dependence of the probability α on the breather height.

We start by quickly reminding that in the MMC model [19] we choose a random triplet of neighboring sites and update their amplitudes under the constraint of constant mass, $a_{n-1} + a_n + a_{n+1} = \bar{a}$, and constant energy, $a_{n-1}^2 + a_n^2 + a_{n+1}^2 = \bar{u}$. These two conditions correspond to the intersection of a sphere with a plane in the three dimensional phase space, a_{n-1}, a_n, a_{n+1}. Since a_n represent a mass it must be positive. This implies that the intersection is a full circle if the initial amplitudes are comparable, while it is made up of three, disconnected arcs if one of the sites has an initial amplitude significantly larger than the others (see Fig. 1(a)). In practice, this occurs when one of the three sites is occupied by a breather.

A first consequence of the results of the previous section is that different microscopic rules for the evolution of the system may produce the same coarsening exponent $1/\zeta$. More specifically, we remind that in Ref. [19] the MMC rule was implemented by restricting the random selection to the fully positive triplets, i.e. choosing points which lie inside the allowed arcs (this could be the entire circle). Here we consider a possible variation of the above dynamics that amounts to always selecting a point along the full circle and accepting the move only if the positivity condition is satisfied for the three amplitudes. Compared to the former recipe, which corresponds to $\alpha = 1$, i.e. $\beta = 0$, the latter algorithm avoids the identification of the arc extrema as functions of the mass and energy of the triplet. On the other hand, the dynamics is slowed down whenever the algorithm generates a triplet with negative amplitudes. Therefore one expects that this change or rule affects the probability α to effectively perturb a breather.

We now show that the slowing down corresponds to $\alpha \sim L^{-1/2}$, i.e. $\beta = 1/2$. Consider a triplet that contains one breather site with amplitude b and two background sites with amplitude xb and yb, with $x, y \ll 1$ and let λ denote the angular length of each arc§. Then, the probability P_a that a randomly chosen move is acceptable is given by the ratio $3\lambda/2\pi$, where the denominator is the amplitude of the set of moves that conserve mass and energy and the numerator accounts for the amplitude of the physical interval (i.e. the set of moves that satisfy also positivity). Since to leading order $\lambda = \sqrt{3}(x+y)$ [19], λ scales as $1/b$ when the background amplitude is kept fixed and then also $P_a \sim 1/b$. Moreover, considering that the quantity diffusing during the MMC dynamics is the energy $u = b^2$ [19], $P_g \sim u^{-1/2}$, so that $\alpha \sim L^{-1/2}$. According to the discussion of previous Section, the difference between the two β exponents, $\beta = 0$ and $\beta = 1/2$, is not sufficient to induce a different coarsening law, which is again characterized by the exponent $\zeta = 1/3$ (data not shown).

Finally, we discuss a modification of the model which naturally leads to an exponentially slow dynamics, without the need to introduce explicitly an exponential decrease of α with L. In practice, we introduce a threshold Γ for the maximal arc length to be considered. In other words, whenever the arc length λ is smaller than Γ, no action is taken: the triplet configuration is left unchanged.

Once again, let us analyse the implications of the algorithm when the chosen triplet contains one breather and two background sites with amplitude b, xb, yb respectively. So long as both x and y are small the dynamics is blocked, since $\lambda = \sqrt{3}(x + y) < \Gamma$. One may naively conclude that sufficiently high breathers are completely decoupled from the background. This is not true, because the background

§ By symmetry reasons the three arcs have the same length λ. When λ equals $2\pi/3$, they merge into the entire circle.

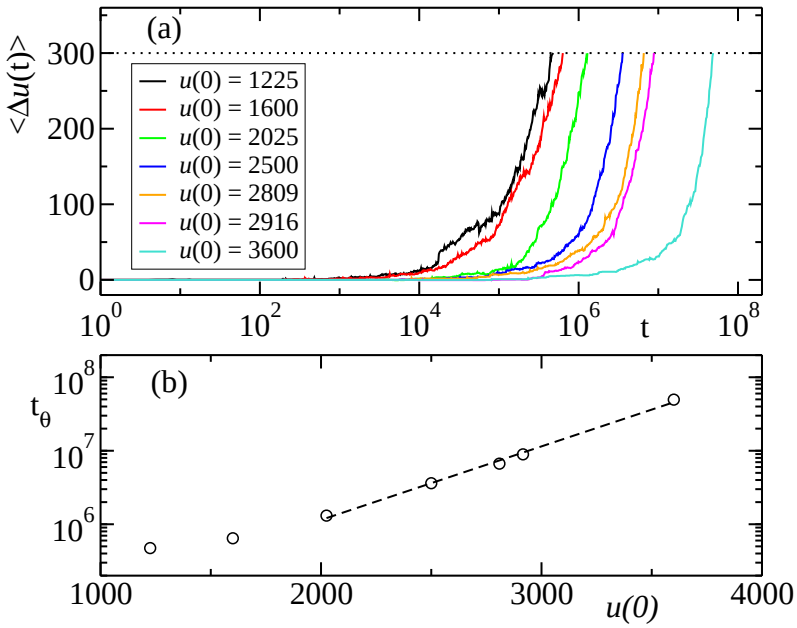

Figure 6. (a): Average energy reduction $\langle \Delta u(t) \rangle \equiv \langle u(0) - u(t) \rangle$ of one breather in a modified MMC model with interaction threshold $\Gamma = \pi/8$ for different initial energies $u(0)$. At $t = 0$ the breather is superposed to an MMC chain in equilibrium at temperature $T = 10$ with mass density $a = 1$ and $L = 2048$. The initial equilibrium distribution of the background is sampled by applying a Metropolis thermostat at $T = 10$ to each site of the chain for a transient $t_{th} = 5 \cdot 10^5$. $\langle \Delta u(t) \rangle$ is computed by averaging over 40 independent trajectories (up to the threshold $\theta = 300$). (b): Relaxation time (open circles) t_θ to reach the threshold as a function of the initial breather energy $u(0)$. The dashed line refers to an exponential fit $t_\theta \sim \exp(u(0)/E)$ with $E = 430$.

fluctuations can eventually lead to sufficiently large x or y values, so that the probability of such move is related to the probability of generating sufficiently large amplitudes in the neighbouring sites. The canonical equilibrium distribution of the background amplitudes a_n reads

$$P(a_n) = \frac{1}{Z} \exp[-\beta(a_n^2 - \mu a_n)], \tag{20}$$

where $\beta = 1/T$ and μ are the inverse temperature and the chemical potential of the system, while $Z = \int_0^\infty \exp[-\beta(a_n^2 - \mu a_n)]\, da_n$ is the partition function. The probability to have a mass fluctuation comparable to the breather height b (the square root of the energy) is exponentially small in b and depends on the values of β and μ. In fact, a direct simulation of the modified MMC model with $\Gamma = \pi/8$ (see Fig. 6(a)), shows that breathers well above the interaction threshold evolve according to an effective coupling exponentially small in the breather energy.

With reference to the parameters of Fig. 6, $\beta = 0.1$ and $\mu = -6.46$ ‖. In the range of chosen breather energies ($u(0) > 1000$), the term in μ in $P(a_n)$ can be

‖ The chemical potential μ has been determined by solving the equation $a = \int_0^\infty P(x) x\, dx$ with $\beta = 0.1$ and $a = 1$.

neglected, so that the probability of the fluctuation is controlled by the local energy a_n^2. This is confirmed in Fig. 6(b), where the relaxation time t_θ necessary to release an amount of energy θ from the breather to the background is shown to depend exponentially on the initial breather energy $u(0)$. Altogether, the above analysis shows that an exponentially small coupling between breathers and background may arise as a consequence of background fluctuations when energy diffusion is blocked by additional constraints. In this regime, the analysis of the previous section predicts a logarithmic coarsening of the breathers.

5. Conclusions

We have investigated the relaxation processes of simple stochastic models, in the perspective of better understanding the dynamics of breathers in the DNLS equation. Our models, the continous MMC and the discrete PEP one, are characterized by a negative temperature region where breathers exchange matter, leading to a decrease of their density. This coarsening process follows a power-law and it is more or less slow, depending in a non trivial way on the strength of the breather-background interaction. In fact, our results and general considerations on the DNLS equation support the idea that the extremely slow dynamics observed in DNLS (an almost frozen dynamics) is due to the weakening of the interaction with breathers of increasing height. However, a power law weakening of the breather-background coupling maintains a power-law coarsening. For this reason, the results of section 4 are particularly instructive. There, we have studed a variant of MMC characterized by a frozen dynamics below some threshold and our results indicate that the invoked *effective* strength may be the outcome of a highly intermittent process. This perspective can plausibly apply to the DNLS, where a resonant interaction of a breather with a neigbouring site could be the motivation for an occasional, localized, strong transfer of energy.

Appendix A. Diffusion with a single semi-reflecting boundary

We want to solve the diffusion equation,

$$\frac{\partial p}{\partial t} = D\frac{\partial^2 p}{\partial x^2}, \tag{A.1}$$

in the semi-infinite line $x \geq 0$, with a semi-reflecting boundary in $x = 0$,

$$\left.\frac{\partial p}{\partial x}\right|_{x=0} = rp(x=0,t), \tag{A.2}$$

and with initial condition $p(x, t = 0) = \delta(x - x_0)$. We remind that within the PEP model, we have $r = 2\alpha$, see Eq. (9).

We define $q(x,t) = p'(x,t) - rp(x,t)$, where the prime indicates the derivative with respect to x, which still satisfies the diffusion equation (A.1), but with the easier boundary condition, $q(0,t) = 0$. The price to be paid is in the initial condition, $q(x,0) = \delta'(x - x_0) - r\delta(x - x_0)$. The details of the calculation can be found in Ref. [27] and here we limit to write the solution

$$\begin{aligned} q(x,t) = & -\frac{1}{\sqrt{4\pi(Dt)^3}}\left[(x+x_0)e^{-\frac{(x+x_0)^2}{4Dt}} + (x-x_0)e^{-\frac{(x-x_0)^2}{4Dt}}\right] \\ & -\frac{r}{\sqrt{4\pi Dt}}\left[e^{-\frac{(x-x_0)^2}{4Dt}} - e^{-\frac{(x+x_0)^2}{4Dt}}\right] \end{aligned} \tag{A.3}$$

and

$$p(x,t) = -\int_x^\infty q(s,t)e^{-r(s-x)}ds. \tag{A.4}$$

What we need is the probability $F(t)$ that the particle is absorbed in $x=0$ during the time interval $(t, t+dt)$, which is given by

$$F(t) = Dp'(0,t) = Drp(0,t) = -Dr\int_0^\infty q(x,t)e^{-rx}dx. \tag{A.5}$$

Therefore, using (A.3) we obtain

$$F(t) = Dr\int_0^\infty dxe^{-rx}\left\{\frac{1}{\sqrt{4\pi(Dt)^3}}\left[(x+x_0)e^{-\frac{(x+x_0)^2}{4Dt}} + (x-x_0)e^{-\frac{(x-x_0)^2}{4Dt}}\right]\right.$$
$$\left. + \frac{r}{\sqrt{4\pi Dt}}\left[e^{-\frac{(x-x_0)^2}{4Dt}} - e^{-\frac{(x+x_0)^2}{4Dt}}\right]\right\}. \tag{A.6}$$

We now formally evaluate the previous integral, which may be written in terms of the error function, $\mathrm{erf}(x) = \frac{2}{\sqrt{\pi}}\int_0^x e^{-s^2}ds$. Then, we evaluate the limiting behaviors of $F(t)$, at short and long times. We need to calculate the following integrals,

$$I_1(x_0) = \int_0^\infty dxe^{-rx}e^{-\frac{(x+x_0)^2}{4Dt}} \tag{A.7}$$
$$= e^{rx_0}\sqrt{\pi Dt}\; e^{r^2Dt}\left[1-\mathrm{erf}\left(r\sqrt{Dt}+\frac{x_0}{2\sqrt{Dt}}\right)\right] \tag{A.8}$$
$$= e^{rx_0}\sqrt{\pi Dt}\; J_1(x_0,r,t) \tag{A.9}$$

where

$$J_1(x_0,r,t) \equiv e^{r^2Dt}\left[1-\mathrm{erf}\left(r\sqrt{Dt}+\frac{x_0}{2\sqrt{Dt}}\right)\right] \tag{A.10}$$

and

$$I_2(x_0) = \int_0^\infty dxe^{-rx}(x+x_0)e^{-\frac{(x+x_0)^2}{4Dt}} \tag{A.11}$$
$$= -e^{rx_0}\sqrt{\pi Dt}\frac{\partial}{\partial r}J_1(x_0,r,t), \tag{A.12}$$

so that

$$F(t) = -\frac{r}{2t}\left[e^{rx_0}\partial_r J_1(x_0,r,t) + e^{-rx_0}\partial_r J_1(-x_0,r,t)\right] \tag{A.13}$$
$$+\frac{Dr^2}{2}\left[e^{rx_0}J_1(x_0,r,t) - e^{-rx_0}J_1(-x_0,r,t)\right]. \tag{A.14}$$

• Limit $x_0^2 \ll Dt \ll r^{-2}$

Using the limit $\mathrm{erf}(x) \simeq \frac{2}{\sqrt{\pi}}x$ for $x \ll 1$, we can write

$$J_1(x_0,r,t) \simeq 1 - \frac{2}{\sqrt{\pi}}\left(r\sqrt{Dt}+\frac{x_0}{2\sqrt{Dt}}\right) \tag{A.15}$$
$$\partial_r J_1(x_0,r,t) \simeq -\frac{2}{\sqrt{\pi}}\sqrt{Dt} \tag{A.16}$$

and

$$F(t) \simeq \frac{2}{\sqrt{\pi}}\sqrt{D}\frac{r}{\sqrt{t}}. \tag{A.17}$$

• Limit $t \gg r^{-2}$

Using the limit $\mathrm{erf}(x) \simeq 1 - \frac{e^{-x^2}}{\sqrt{\pi}x}$ for $x \gg 1$, we can write

$$J_1(x_0, r, t) \simeq \frac{1}{r\sqrt{\pi D t}} \tag{A.18}$$

$$\partial_r J_1(x_0, r, t) \simeq -\frac{1}{r^2\sqrt{\pi D t}} \tag{A.19}$$

and

$$F(t) \simeq \frac{1}{r\sqrt{\pi D}} t^{-3/2}. \tag{A.20}$$

Using $r = 2\alpha$, from (A.17) and (A.20), we find Eqs. (10).

Appendix B. Relaxation of a breather on an empty background

• Limit $x_0^2 \ll t \ll \alpha^{-2}$

Recalling that

$$\int_0^\infty dt F(t) = 1 \quad , \tag{B.1}$$

we rewrite Eq. (11) as

$$\langle \Delta h(t) \rangle = \alpha \int_0^t dt' (1 - p_1(t')) \left[1 - \int_0^{t'} dt'' F(t'') \right]. \tag{B.2}$$

Now, since at short times

$$\int_0^{t'} dt'' F(t'') \ll D^{1/2} \simeq 1 \tag{B.3}$$

and $p_1 \ll 1$, we obtain to the leading order

$$\langle \Delta h(t) \rangle = \alpha t. \tag{B.4}$$

• Limit $t \gg \alpha^{-2}$

Let us introduce an intermediate timescale t_0 such that $\alpha^{-2} \ll t_0 \leq t$. Therefore, Eq. (11) is rewritten as

$$\langle \Delta h(t) \rangle = \alpha \left[\int_0^{t_0} dt' (1 - p_1(t')) \int_0^{t'} dt'' F(t'') + \int_{t_0}^t dt' (1 - p_1(t')) \int_0^{t'} dt'' F(t'') \right]. \tag{B.5}$$

In the regime $t \gg \alpha^{-2}$, $F(t)$ can be approximated as in Eq. (10) and $p_1(t) \simeq 1/2$. Consequently, one can compute explicitly the second addend in the square brackets, that gives

$$\int_{t_0}^t dt' (1 - p_1(t')) \int_0^{t'} dt'' F(t'') = \frac{1}{2} \int_{t_0}^t dt' \int_0^{t'} dt'' \frac{1}{2\alpha\sqrt{\pi D t''^3}} = \frac{1}{\alpha} \sqrt{\frac{t}{\pi D}}. \tag{B.6}$$

Therefore, for $t \geq t_0$

$$\langle \Delta h(t) \rangle = K(t_0) + \sqrt{\frac{t}{\pi D}}, \tag{B.7}$$

where $K(t_0)$ is a constant. Finally, for $D = 1/2$, we obtain Eq. (13).

Appendix C. Random walk with two semi-reflecting boundaries

We have two breathers in $i = 0, L$ and a random walk in between, moving according to the following rules: if the particle is in $i \neq 1, L-1$, it hops to $i \pm 1$ with probability $1/2$; if $i = 1$ ($i = L-1$), it hops to $i = 2$ ($i = L-2$) with probability q and to $i = 0$ ($i = L$), therefore being absorbed, with probability $1-q$. We define the probability $P(L)$ that a particle released in $i = 1$ attaches to the breather in $i = L$.

It is also useful to define a model where the left boundary condition is the same as before, but the right boundary condition is symmetric, i.e. the particle hops from $i = L-1$ to $i = L-2, L$ with probability $1/2$. For this model we define the probability $p(L)$ that a particle released in $i = 1$ reaches the site $i = L$ before reaching the site $i = 0$. With these notations, we can write

$$P(L) = p\left(\frac{L}{2}\right)\frac{1}{2}, \tag{C.1}$$

because a particle arrived in $L/2$ has the same probability to attach to the left or to the right breather. We now want to determine $p(L)$, summing up all the possible trajectories to go from $i = 1$ to $i = L$, without being absorbed in $i = 0$, according to the number n of passages in $i = 1$ (with $n \geq 1$). If a trajectory is characterized by a given n, it means that the particle has hopped from 1 to 2 (which happens with probability q) and $(n-1)$ times it has come back to 1 before attaining L (which occurs with probability $(1-a)$, with $a = 1/L$), and one time has attained L before coming back to 1 (which occurs with probability a). Summing up all terms, we have

$$p(L) = \sum_{n\geq 1} q^n (1-a)^{n-1} a \tag{C.2}$$

$$= \frac{a}{1-a}\sum_{n} q^n (1-a)^n \tag{C.3}$$

$$= \frac{aq}{(1-q)+qa}, \tag{C.4}$$

with $a = 1/L$. So, we get

$$P(L) = p\left(\frac{L}{2}\right)\frac{1}{2} \tag{C.5}$$

$$= \frac{q}{2q + L(1-q)} \tag{C.6}$$

$$= \frac{1}{2 + L(q^{-1}-1)}. \tag{C.7}$$

Let us now define q in the most general way. If a particle is in $i = 1$, it has a probability $1/4$ to move to the right and a probability $\alpha/2$ to move to the left,¶ so

$$q = \frac{\frac{1}{4}}{\frac{1}{4} + \frac{\alpha}{2}} = \frac{1}{1+2\alpha}, \tag{C.8}$$

and

$$P(L) = \frac{1}{2}\frac{1}{1+L\alpha}. \tag{C.9}$$

¶ Each probability is the product of $1/2$ (the probability to choose right or left) with the probability to actually make the move.

References

[1] Eilbeck J, Lomdahl P and Scott A 1985 Physica D **16** 318–338
[2] Kevrekidis P G 2009 The Discrete Nonlinear Schrödinger Equation (Springer Verlag, Berlin)
[3] Tsironis G and Hennig D 1999 Phys. Rep. **307** 333–432
[4] Trombettoni A and Smerzi A 2001 Physical Review Letters **86** 2353
[5] Hennig H, Neff T and Fleischmann R 2016 Physical Review E **93** 032219
[6] Franzosi R, Livi R, Oppo G and Politi A 2011 Nonlinearity **24** R89
[7] Jensen S 1982 Quantum Electronics, IEEE Journal of **18** 1580–1583
[8] Christodoulides D and Joseph R 1988 Optics letters **13** 794–796
[9] Rumpf B and Newell A C 2001 Physical Review Letters **87**
[10] Borlenghi S, Wang W, Fangohr H, Bergqvist L and Delin A 2014 Physical review letters **112** 047203
[11] Borlenghi S, Iubini S, Lepri S, Chico J, Bergqvist L, Delin A and Fransson J 2015 Physical Review E **92** 012116
[12] Flach S and Gorbach A V 2008 Physics Reports **467** 1–116
[13] Rasmussen K, Cretegny T, Kevrekidis P and Grønbech-Jensen N 2000 Phys. Rev. Lett. **84** 3740–3743
[14] Iubini S, Franzosi R, Livi R, Oppo G L and Politi A 2013 New Journal of Physics **15** 023032
[15] Rumpf B 2004 Phys. Rev. E **69** 016618
[16] Rumpf B 2007 EPL (Europhysics Letters) **78** 26001
[17] Rumpf B 2008 Physical Review E **77** 036606
[18] Rumpf B 2009 Physica D: Nonlinear Phenomena **238** 2067–2077
[19] Iubini S, Politi A and Politi P 2014 Journal of Statistical Physics **154** 1057–1073
[20] Kuramoto Y 2012 Chemical oscillations, waves, and turbulence vol 19 (Springer Science & Business Media)
[21] Krapivsky P L, Redner S and Ben-Naim E 2010 A kinetic view of statistical physics (Cambridge University Press)
[22] Edwards S F and Wilkinson D 1982 The surface statistics of a granular aggregate Proceedings of the Royal Society of London A: Mathematical, Physical and Engineering Sciences vol 381 (The Royal Society) pp 17–31
[23] Basile G, Bernardin C and Olla S 2006 Phys. Rev. Lett. **96** 204303
[24] Lepri S, Mejía-Monasterio C and Politi A 2009 J. Phys. A: Math. Theor. **42** 025001
[25] Lepri S, Mejía-Monasterio C and Politi A 2010 Journal of Physics A: Mathematical and Theoretical **43** 065002
[26] Delfini L, Lepri S, Livi R, Meja-Monasterio C and Politi A 2010 J. Phys. A: Math. Theor. **43** 145001
[27] Weiss G H 1994 Aspects and applications of the random walk (Amsterdam: North-Holland)